Appointment Scheduling for Medical Diagnostic Centers considering Time-sensitive Pharmaceuticals: A Dynamic Robust Optimization Approach

Mohammad Mahdavi Mazdeh*

School of Industrial Engineering, Iran University of Science and Technology, Tehran, Iran

Mohammad Namakshenas

School of Industrial Engineering, Iran University of Science and Technology, Tehran, Iran

Aleida Braaksma

Center for Healthcare Operations Improvement and Research (CHOIR), University of Twente, Enschede, The Netherlands

Mahdi Heydari

School of Industrial Engineering, Iran University of Science and Technology, Tehran, Iran

Abstract

This paper studies optimal criteria for the appointment scheduling of outpatients in a medical imaging center. The main goal of this study is to coordinate the assignments of radiopharmaceuticals and the scheduling of outpatients on imaging scanners. We study a special case of a molecular imaging center that offers services for various diagnostic procedures for outpatient requests. Most procedures in molecular imaging require a time-sensitive chemical element, technetium-99m (`99mTc`) with a limited half-life, and involve several steps that are constrained by strict time windows. The most important component of the radiopharmaceuticals produced in a molecular imaging center is `99mTc`. We investigate the mathematical dynamics of `99mTc` dosages to construct optimal schedules for preparing the radiopharmaceuticals. We develop a rigorous mixed-integer programming model to coordinate the assignment of the radiopharmaceuticals and the scheduling of outpatients on the scanners. The objective is to minimize the total deviation from the scheduled scanning times. We also develop a novel, less conservative robust optimization approach to capture the uncertainty raised by the availability of `99mTc`. We propose an uncertainty handling mechanism to recursively reduce the uncertainty interval over time. The proposed mechanism avoids over-conservatism and increase the reliability of mathematical robust models. We evaluate the proposed models by multiple criteria. The final results suggest that the robust model is able to schedule up to 40 outpatients with at most 20 percent of deviation from the scheduled scan times versus 30 outpatients with at most 50 percent according to the current practice. The other criteria, such as the degree of the constraint violation, suggest that the proposed model is practical and consistent with the clinical requirements.

Keywords: Healthcare, Medical imaging, Scheduling, Outpatient appointment, Mixed integer programming, Robust optimization

1. Introduction

The increased demand for medical imaging and diagnostic centers has been recognized as one of the contributors to the rise of health care costs in the world in the last few years [1]. In this research, we study a molecular imaging case, which is helpful for studying the structural and functional details of any organ system, detecting diseases in early stages and extent of disease and applying a targeted therapy. Current clinical molecular imaging protocols primarily use single-photon emission computed tomography (SPECT) scanners and radiopharmaceuticals. The decay product of molybdenum-99 (`99Mo`), i.e., technetium-99m (`99mTc`), comprises 80 percent of all molecular procedures representing over 30 million procedures worldwide each year [2, 3]. It is a convenient gamma-ray emitting isotope with a half-life of 6 hours and it is available in the form of `99Mo`/`99mTc`-generators. For notational simplicity, we abbreviate the term `99Mo`/`99mTc`-generator as `MT-G`. The process of extracting `99mTc` is called *elution*.

Globally, molecular imaging investigations are the second most common diagnostic imaging procedure after computer tomography (CT). On a global scale, over 28 million procedures are carried out each year by means of `99mTc`. The majority of the procedures are for cardiac and bone imaging. Procedures in molecular imaging require the use of radiopharmaceuticals which are mainly derived from `99mTc`, a daughter product of `99Mo`. The chemical attributes of `99mTc`[1] have made it popular for most molecular imaging procedures. However, in recent years, `99Mo` has become expensive and its routine availability can no longer be taken for granted [1].

Managing outpatient services in a molecular imaging center is a very challenging problem that has received little research attention. The short half-life of the radiopharmaceuticals produced by the `MT-G` process imposes strict temporal constraints on scheduling patients. Suthummanon et al. [4] showed that administrating scanners and radiopharmaceuticals account for most of the expenses per procedure. The main goal of this research is to design optimal scheduling policies for patients and to develop efficient elusion scenarios while maintaining the diagnostic accuracy of tests. The side benefit of such a policy is that it reduces radiation exposure to patients.

In this study, we consider the case of SPECT scanning protocols in a molecular imaging department that offers services for a myriad of diagnostic procedures for outpatient requests. Section 2 offers a brief review of the literature on administrating medical imaging centers, especially molecular centers. Section 3 introduces the detailed problem description. We address three major concerns in this study. First, Section 4 discusses scenarios for dose management of eluted `99mTc` considering the dynamics of `MT-G` from the viewpoint of mathematical formalism and optimality analyses. Second, Section 5 focuses on scheduling the procedures of individual patients: reduction in total procedure

*Corresponding author
Email address: `mazdeh@iust.ac.ir` (Mohammad Mahdavi Mazdeh)

[1] a short half-life, no particulate radiation, cheap, and readily available

time as a service, low-exposure to radiation as a health concern, optimal allocation of radiopharmaceuticals as a reduction of costs and environmental problems, and increasing the image quality as a reduction in staff workload. Third, Section 6 introduces a novel dynamic robust optimization framework to handle the uncertainty in the amount of eluted ^{99m}Tc.

2. Literature Review

In this section, we overview several important studies from both administrating radiopharmaceuticals and scheduling appointments in medical imaging centers. Andersson and Mattsson [5] investigated various approaches, from clinical and practical methods to theoretical physics analytical tools, to manage the dosage in a molecular imaging center. They also stressed the concern with absorbed dosage and therewith the risks associated with radiation. Their main advice towards optimizing the dosage was to adjust the administered activity by the patient's weight. Nagurney and Nagurney [6] and Nagurney et al. [7] tackled the problem of a global shortage in ^{99}Mo by strategic network analysis of the ^{99}Mo supply chain in the world, i.e., production, transportation, purification, manufacturing, and elucitation. They exploited the physics principles to determine the loss, due to time-decay, of the radioisotope on the various links of the supply chain network and developed a generalized network optimization model.

The existing literature on scheduling molecular imaging clinics is limited. It appears that most of the studies for specialty clinics focus on scheduling CT scan and magnetic resonance imaging (MRI) procedures, which are relatively easy to manage since they do not consider radiopharmaceuticals nor multi-step sequences. Pérez et al. [8] proposed a stochastic online problem, more specifically a two-stage stochastic integer programming model, to find the best day and time to accommodate the current request such that the system's performance measures are improved. They assume that possible future patient medical information is available to make more informed decisions when scheduling patients and resources under uncertainty. The main goal of their study was to provide shorter patient waiting times, increased patient throughput, minimal delays in the delivery of the radiopharmaceuticals, higher utilization of resources, and ultimately lower health care costs.

In another study, Pérez et al. [9] formulated the problem in [8] as a resource-constrained scheduling problem assuming three scenarios: base patient demand, low patient demand, and high patient demand. In this problem, the resource refers to the hospital personnel including technologists. They delivered two algorithms for scheduling patients from the view of both waiting times for the patient and the utilization of resources. The algorithms provided a more balanced utilization of human resources, independent of the demand. The algorithms were able to provide appointments with less waiting times for patients.

Pérez et al. [10] and Roman [11] presented a discrete event system simulation model for a molecular imaging department for patient service management. They investigated the problem by taking into account three main components to perform a successful procedure: a radiopharmaceutical, gamma camera with CT, and technologist and technician. The scanning quality was another concern in this study. If a scan is made too early before the radiopharmaceutical has diffused adequately or too late after excessive decay, it results in a poor image. If there is too much delay, the procedure must be terminated and repeated on another day. This issue causes unnecessary exposure to radiation and increased

costs. One of the important findings of these studies was that assigning technologists to specific stations results in reduced patient throughput. Moreover, reducing workload even by a single technologist can result in scheduling the procedures with high patient demand. Akhavizadegan et al. [12] delivered a Markov decision problem to model resource management, multi-priority patients with different arrival rates and walk-ins, and revenue management in a molecular imaging center. They also assume that the revenue model incurs costs if service to a patient is not satisfactory. They concluded that the add up in capacity contributes to the growth of the total net revenue and the decrease in waiting costs.

Because the literature on scheduling molecular imaging clinics is limited, we also discuss some of the important works from the related areas of scheduling CT and MRI scans. Patrick and Puterman [13] postulated that the key rule to manage and schedule patients is to classify them into priorities based on their emergency level. With emergency patients arriving randomly, the main question is: how should non-emergency patients be scheduled to realize an even and smooth workload? They formulated the model via a Markov decision process from the highest workload state to the lowest possible workload state. Next, they approximated the emerged model with linear programming and also developed a column generation algorithm to efficiently solve the linear programming model. Patrick et al. [14], in a similar study, classified the requests into low and high priority requests in a CT center. They compared their revenue model with that of an airline. The final results indicated that inserting one day delay after processing ten percent of inpatients causes a significant reduction in waiting times' growth rate. Green et al. [15] proposed to categorize patients into inpatient, outpatient, and emergency groups. They also developed a revenue model to balance the income dominance between inpatients and outpatients and waiting time costs of outpatients. Berg and Denton [16] proposed a two-stage mathematical model to decide the scheduling of emergency patients in one stage and outpatients in another stage.

Our study differs from the previous works in the way that we consider the dynamics of `99mTc` and build practical and optimal scenarios to efficiently model the scheduling problem. To the best of the authors' knowledge, no previous study has addressed the uncertainty in the amount of eluted `99mTc`. The remainder of this paper is organized as follows. In Section 3, we describe the operational details of a complete molecular imaging procedure with the corresponding mathematical notations. Section 4 proposes several practical scenarios to manage the dosage effectively. Section 5 develops a mixed integer programming model to schedule a complete procedure. Section 6 proposes a novel robust optimization approach to protect the uncertainty-affected constraints against the worst-case scenarios. In Section 7, we apply the complete mathematical model to our case study instance. We study the case of a molecular imaging center in the Shariati hospital located in Tehran, Iran. In our case study, the appointments are scheduled for one week ahead and a specific number of patients are scanned in the center during a week. We study five important and most frequent procedures processed on six different scanners. The last section concludes the study with a summary and suggestions for future research.

3. Problem Description

Prior to discussing the details of the problem, let us review some important terms and how different entities in molecular imaging are connected. A typical imaging procedure

requires at least three entities: a radiopharmaceutical, a SPECT scanner equipped with a gamma camera, and a nurse or technician.

A radiopharmaceutical is a combination of a non-radioactive compound with a radioactive isotope, a radio-nuclide like `99mTc`. As we discussed before, the radiopharmaceuticals produced by `99mTc` determine the localization and bio-distribution of various body organs. Any radiopharmaceuticals produced by `99mTc` should be delivered to the clinics in a short amount of time; hence, they are prepared using an apparatus called `99Mo-99mTc` generator (`MT-G`) inside the clinic. An `MT-G` consists of a `99Mo` and `99mTc` pair in a well-shielded container that permits separation of `99mTc` which is the decay product of `99Mo`. In other words, the `99mTc` activity is replenished and eluted continuously by the decay of `99Mo`. An `MT-G` is typically in use for approximately one week and then discarded because of the half-life of `99Mo`, about 66 hours. A technician prepares a radiopharmaceuticals by mixing a portion of `99mTc` with a non-radioactive compound according to the procedure's protocol.

The produced radiopharmaceuticals is injected into the patient's bloodstream, and it accumulates in a target organ within a specific time frame w.r.t. the procedure. The scanning process should start close to the end of this time frame so that the quality of the acquired image would be acceptable. A SPECT scanner is an imaging device capable of detecting the signals of radiopharmaceuticals, i.e., a gamma camera in this scanner collects data to create detailed images of cell activities and biological processes. A scan could last from minutes to hours.

Multiple sequential steps have to be initiated and completed within a specific time window to complete a procedure successfully. If the procedure protocol is not managed carefully, a poor scan will result in patient rescheduling. In what follows, we describe the commonalities of a simple procedure at the operational level with the mathematical parameters and decision variables.

Constants

n	Number of patients
m	Number of scanners
q	Number of elution periods
a_{M_0}	`99Mo` activity at time zero
λ_M	Decay rate of `99Mo` and equals $\log(2)/66.02$
λ_T	Decay rate of `99mTc` and equals $\log(2)/6$
c	Numerically large number
h	Maximum number of allowed `99mTc` elutions in a day

Sets

J	Set of all patients, $j \in J = \{1, \ldots, n\}$
Q	Set of elution periods, $k \in Q = \{1, \ldots, q\}$
I	Set of scanners, $i \in I = \{1, \ldots, m\}$
B_i	Set of patients that can be scanned on scanner i

Parameters

g	The branching ratio
u_j	Activity required (mCi[2]) for scanning patient j
b	Duration of preparing and injecting the radiopharmaceutical

[2]Millicurie

w_j Preferred waiting time until starting the scanning of patient j
r Setup time including changing the collimator and configuring a scanner for a different procedure
v_k Activity eluted (mCi) at elution period k
l_k Maximum time for injecting the radiopharmaceutical at elution period k
t_k kth elution time
p_j Scan duration of patient j
$o_{jj'}$ A boolean matrix: 1 if two patients j and j' have the same procedure; 0 otherwise.

Decision Variables

x_{jk} 1 if patient j is allocated to the kth elution period; 0 otherwise.
$s_j^{(1)}$ Start time of injecting patient j
$y_{jj'}^{(1)}$ 1 if patient j' follows patient j in the injection stage (not necessarily immediately); 0 otherwise.
d_j Imposed completion time of scanning patient j
$s_j^{(2)}$ Start time of scanning patient j
$y_{ijj'}^{(2)}$ 1 if patient j immediately precedes patient j' on scanner i; 0 otherwise.
z_{ij} 1 if patient j is allocated to scanner i; 0 otherwise.
E_j Earliness of scanning patient $j = \max\left\{d_j - \left(s_j^{(2)} + p_j\right), 0\right\}$
T_j Tardiness of scanning patient $j = \max\left\{s_j^{(2)} + p_j - d_j, 0\right\}$

First, the technician elutes `99mTc` from the generator and combines it with a non-radioactive compound. The required amount of `99mTc`, u_j mCi, depends on the type of procedure of patient j. The technician is responsible for injecting the patients with the radiopharmaceutical. The technician elutes `99mTc` from the generator q times in a week, at times $t_k,\ k \in Q$. The total activity eluted at time t_k is v_k mCi. The technician should inject the radiopharmaceutical no later than $t_k + l_k$ upon the radiopharmaceutical is prepared. The technician can only inject one patient at a time; however, after the injection, the patients can wait simultaneously in the waiting room to get the pharmaceutical to be absorbed and distributed in the target organ. Hence, the starting time of injection for patient j, $s_j^{(1)}$, should be at least b time units apart. Finally, the patient is ready to be scanned and the preferred starting time for the scan equals $s_j^{(1)}$ plus the injection time b plus waiting time, w_j. The preferred scan start plus scan duration is called the imposed scan completion time, d_j. Any deviation from this preference is not favourable. The patients are assigned to the scanner, z_{ij}, and if a scanner is idle and eligible to scan the procedure of the patient, the scan starts, $s_j^{(2)}$. If patient j is scanned too early, $E_j > 0, T_j = 0$, then the scanned image will be too noisy and the image analysis will be impossible. If patient j is scanned too late, $T_j > 0, E_j = 0$, again, it will result in poor image quality. Hence, the objective is to minimize any deviation from this preferred time (this, by definition, exactly corresponds to a Just-In-Time system in a production environment). This can be done by minimizing over equation $\sum_{j \in J}(E_j + T_j)$, i.e., the total deviation from imposed scan completion times.

Not all scanners are able to handle all types of procedures. Many SPECT studies are combined with computed tomography (CT) studies to obtain accurate localization. This type of scanner is known as SPECT-CT. The scanners and the procedures are connected

through set B_i. One of the challenges that a molecular imaging center could face is to minimize the assignment of sequential different procedures to the same scanner, because, a setup time, r, is required to change the collimator, the detector of the scanner, and configuring the software of the scanner according to a specific procedure. We impose a sequence-independent setup time when two patients with different procedures are assigned to the same scanner and processed one after another (see set $o_{jj'}$).

4. Dynamics of Resource

In this section, our focus is on the mathematical dynamics of molybdenum-99/technetium-99m (`99Mo/99mTc`). In practice, it is not possible to elute the `MT-G` at arbitrary times of a day. The `99mTc` activity reaches a maximum after approximately 23 hours inside the `MT-G`, at which time the production rate and the decay rate are equal and the `99mTc`, with decay rate λ_T, and the `99Mo`, with decay rate λ_M, pair are said to be in the transient equilibrium. Once the transient equilibrium is achieved, the `99mTc` activity decreases by about the half-life of `99Mo`. In theory, the `99mTc` activity will exceed `99Mo` after passing this equilibrium. Equation 1, also known as the reduced form of the Bateman equation [17] for paired parent/daughter isotopes, captures the transient equilibrium for such a pair. Variable $a_T(t)$ computes the eluted activity of `99mTC` at time t measured by a depreciating metric called millicurie (mCi).

$$\begin{aligned} \theta &= a_{M_0} \frac{\lambda_M}{\lambda_M - \lambda_T} \\ a_T(t) &= \theta \left(e^{-\lambda_M t} - e^{-\lambda_T t} \right) \end{aligned} \tag{1}$$

Equation 1 does not accurately compute the amount of `99mTc` in individual elutions since the `MT-G` does not yield a hundred percent of the available activity in practice. The ratio of `99mTc` decay into 99Mo activity inside the `MT-G` in the state of transient equilibrium, also known as the branching ratio, is approximately $g = 0.86$. The theoretical versus the practical states are illustrated in Figure 1. We deduce a recursive function to compute the practical build-up activity at the kth elution period in Proposition 1. Note that, in this section, we temporarily assume that v_k and t_k are decision variables.

Proposition 1. *Assuming q elution periods, the recursive function to determine the activity in the kth elution is computed as follows,*

$$\begin{aligned} \theta = \frac{a_{M_0} g \lambda_M}{\lambda_M - \lambda_T}, \quad t_0 = 0 \\ v_k = \theta e^{-\lambda_M t_{k-1}} \left(e^{-\lambda_M (t_k - t_{k-1})} - e^{-\lambda_T (t_k - t_{k-1})} \right), \quad k \in Q. \end{aligned} \tag{2}$$

Proof. It suffices to compute the activity of `99Mo` at the $(k-1)$th elution, i.e., $a_{M_0} e^{-\lambda_M t_{k-1}}$, and the decayed activity during $(t_k - t_{k-1})$. By plugging these into Equation 1, we construct the recursive function. □

Note that the efficiency may vary from one elution to the next (Figure 2). Moreover, we are mainly interested in the maximum activity build-up disregarding the scheduling preferences; precisely, maximizing over $\sum_k v_k$. The only purpose is to find the interval

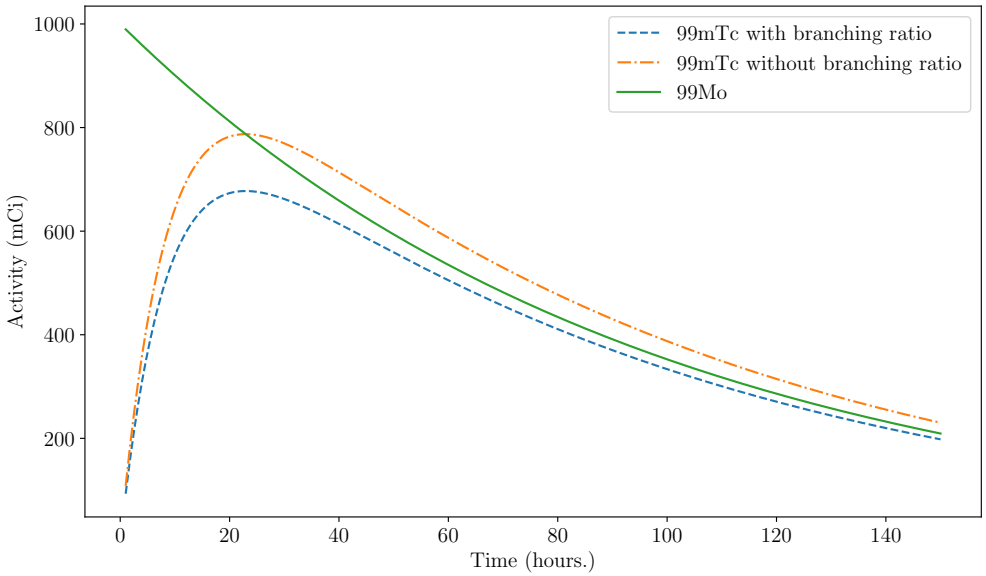

Figure 1: Transient equilibrium inside `MT-G` ($a_{M_0} = 1000$)

between elutions and developing the elution vector, t. In what follows, we first investigate the optimality conditions for the build-up function.

$$\begin{aligned} &\max_{\mathbf{t}\in\mathbb{R}_+} \mathbf{F}(\mathbf{t}) \\ &F(t) = \theta \sum_{k=0}^{q-1} e^{-\lambda_M t_k} \left(e^{-\lambda_M (t_{k+1}-t_k)} - e^{-\lambda_T (t_{k+1}-t_k)} \right) \\ &G_k(t) = -t_k \leq 0, \quad \forall k \in \{1, \ldots, q\} \end{aligned} \tag{3}$$

Theorem 4.1. *$F(t)$ is neither convex nor concave for $t \in \mathbb{R}_+$.*

Proof. $F(t)$ can be rearranged as follows,

$$\begin{aligned} F_1(t) &= \left(e^{-\lambda_M t_1} + \sum_{k=2}^{q} e^{-\lambda_T t_k} \right) \\ F_2(t) &= \left(e^{-\lambda_T t_1} + \sum_{k=1}^{q-1} e^{-t_k(\lambda_M - \lambda_T) - \lambda_T t_{k+1}} \right) \\ F(t) &= \theta \left(F_1(t) - F_2(t) \right). \end{aligned} \tag{4}$$

Expressions $e^{-\lambda_M t_1}$, $e^{-\lambda_T t_1}$, and $e^{-\lambda_T t_k}$, $\forall k \in \{2, \ldots, q\}$ are all twice differentiable posi-

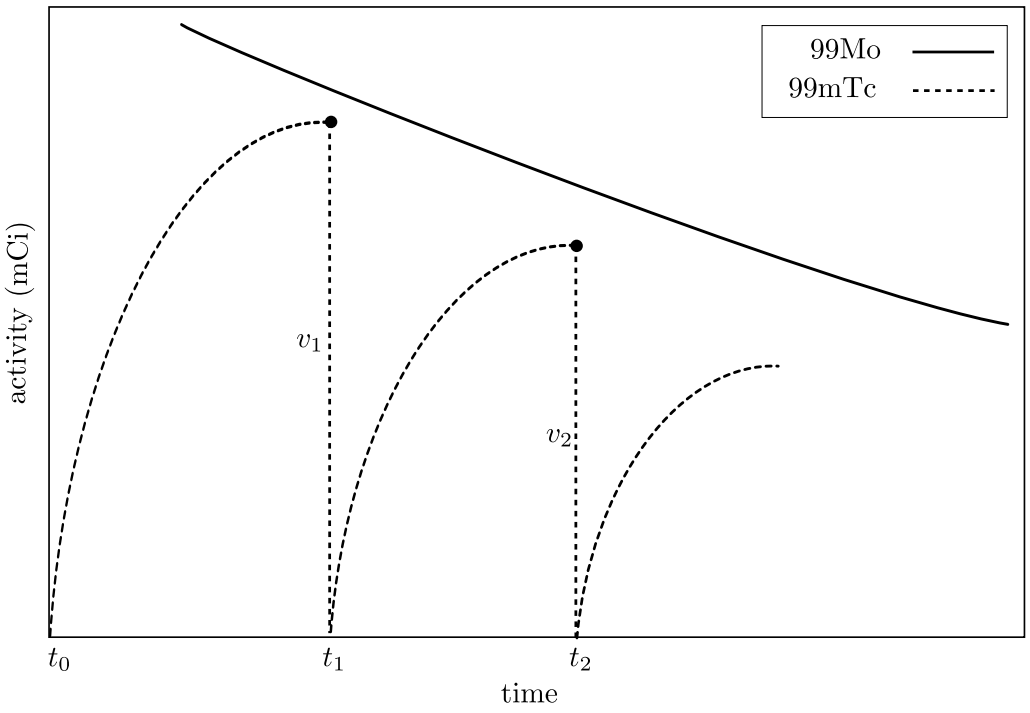

Figure 2: Activity build-up inside `MT-G` w.r.t. elution vector

tive functions and are immediately convex. Expression $\sum_{k=2}^{q} e^{-\lambda_T t_k}$ is also convex since the sum of convex functions is convex. The convexity of expression $\sum_{k=1}^{q-1} e^{-t_k(\lambda_M-\lambda_T)-\lambda_T t_{k+1}}$ can also be verified based on the argument that the product of two positive convex functions, i.e., $e^{-t_k(\lambda_M-\lambda_T)}$ and $e^{-\lambda_T t_{k+1}}$, is also convex. Hence, $F_1(t)$ and $F_2(t)$ are convex functions; however, there is no guaranteed convexity or concavity property for $F(t)$. Intuitively, a counterexample can be constructed given $q = 2$ by evaluating the eigenvector for the Hessian at $t_1 = 500$ and $t_2 = 3000$. Then, the eigenvector is $(-0.000234, 0.00009848)$. The results follow directly. □

The necessary Karush–Kuhn–Tucker (KKT) conditions can be checked as follows,

$$\begin{aligned} &\frac{\partial F(t^*)}{\partial t_k} + \mu_k = 0, \quad \forall k \in \{1, \ldots, q\} \\ &t_k \geq 0,\ \mu_k \geq 0 \quad \textbf{or} \quad t_k > 0,\ \mu_k = 0, \quad \forall k \in \{1, \ldots, q\} \end{aligned} \tag{5}$$

The locally optimal elution vector, t^*, verifying the KKT necessary condition can be found by non-linear searching methods. However, the following theorem makes use of the KKT sufficient conditions [18] for the generalized convexity to provide the certificate that the candidate solution satisfying the KKT's necessary condition is also globally optimal.

Theorem 4.2. *Any locally optimal elution vector, t^*, satisfying the KKT necessary*

condition is also globally optimal for $\lambda_T \geq \lambda_M$.

Proof. According to the principle of KKT sufficient conditions for the generalized convexity, it suffices to check that $F(t)$ is pseudo-concave. Hence, we have,

$$(\lambda_T - \lambda_M)e^{-(\lambda_M-\lambda_T)t_k-\lambda_T t_{k+1}}(t'_k - t_k) \leq 0 \quad \Longrightarrow \quad F(t') \leq F(t), \quad \forall k \in \{0,\ldots,q-1\}. \tag{6}$$

By assuming $\lambda_T \geq \lambda_M$, expression $(\lambda_T - \lambda_M)e^{-(\lambda_M-\lambda_T)t_k-\lambda_T t_{k+1}}$ is a non-negative function and it is immediate that $t'_k \leq t_k$, $\forall k$. This directly implies that $F(t)$ is a monotonically non-decreasing function. The results follow directly. □

Example 1. Given $q = 1$ the local solution $t_1^* = {}^{\theta(\log(\lambda_T)-\log(\lambda_M))}/_{(\lambda_T-\lambda_M)}$ necessarily satisfies the KKT condition. It immediately verifies that $F(t)$ is concave, thus pseudo-concave (this result only holds for case $q = 1$). We provide the optimal elution vectors up to $q = 5$ in Table 1.

Table 1: Optimal elution vectors evaluated for up to $q = 5$ with initial activity $a_{M_0} = 1000$ mCi

q	Optimal elution vector (t^***hour**, v^***mCi**)					$F(t^*)$ **mCi**
	1	2	3	4	5	
1	(22.94,677.39)					677.39
2	(17.78,663.84)	(40.72,562.72)				1226.56
3	(15.00,640.85)	(32.78,567.71)	(55.72,481.23)			1689.79
4	(13.15,616.70)	(28.15,558.70)	(45.93,494.95)	(68.87,419.56)		2089.89
5	(11.80,593.36)	(24.95,545.29)	(39.95,494.00)	(57.73,437.63)	(80.67,370.97)	2441.24

In order to form realistic elution decisions, we should consider clinical guidelines as follows,

- The life cycle of an `MT-G` is about 5 days. All elutions should be distributed within these 5 days.
- The plan should contain one elution at 7:00 morning every day.
- The minimum eluted activity cannot be less than the maximum required activity of a procedure on a certain day.
- All elutions should be conducted between 7:00 and 11:00 on each day. This is partly due to the preparation protocols such as being sober and reasonable time to prepare the pharmaceutical.

Hence, we formulate a maximization model based on the above guidelines,

$$
\begin{aligned}
\max_{t,v\in\mathbb{R}_+} \quad & \theta\sum_{k=1}^{q} v_k \\
\text{s.t.} \quad & \\
& v_k = e^{-\lambda_M t_k}\left(e^{-\lambda_M(t_k-t_{k-1})} - e^{-\lambda_T(t_k-t_{k-1})}\right), \quad \forall k \in \{1,\dots,q\}, \\
& t_k \le \lceil k/h \rceil\, \beta + (11-7), \quad \forall k \in \{1,\dots,q\}, \\
& t_k \ge \lceil k/h \rceil\, \beta, \quad \forall k \in \{1,\dots,q\}, \\
& t_{k+1} - t_k \ge 1, \quad \forall k \in \{1,\dots,q-1\}, \\
& v_k \ge \max_{j\in J}\{u_j\}, \quad \forall k \in \{1,\dots,q\}, \\
& t_0 = 0.
\end{aligned} \tag{7}
$$

where β equals ${\theta\left(\ln(\lambda_T)-\ln(\lambda_M)\right)}/{(\lambda_T-\lambda_M)}$ and h denotes the number of elutions in a day.

Proposition 2. *Any locally optimal elution vector, t^*, satisfying the KKT necessary condition is also globally optimal for optimization problem 7 such that $\lambda_T \ge \lambda_M$.*

Proof. In Theorem 4.2, we proved that the objective function of problem 7 is pseudo-concave. The constraints of problem 7 are also linear, thus quasi-convex. The result follows directly. □

We solve problem 7 by setting $q = 10$, $a_{M_0} = 1000$, and $h = 2$ and illustrate the results in Figure 3

5. Mixed Integer Programming Model

In this section, we formulate the problem in several sets of constraints and an objective given the elution vector t and v as inputs from the previous section. The mixed integer programming (MIP) model is based on offline scheduling, i.e., the scheduling of all appointments must be made a finite time prior to the start of a clinic session. The model does not incorporate emergency requests, no-shows, unpunctual patients, and walk-ins. Since the life cycle of each `MT-G` is approximately one week, the planning period is considered to be 5 days, excluding the weekends. In what follows, we describe the MIP model constraint-wise step by step.

Constraints set 8 assigns a patient to only one elution period,

$$\sum_{k\in Q} x_{jk} = 1, \quad \forall j \in J. \tag{8}$$

The following constraint set 9 guarantees that total activity required for a set of selected patients in elution period k does not exceed the total eluted volume in that period.

$$\sum_{j\in J} u_j x_{jk} \le v_k, \quad \forall k \in Q. \tag{9}$$

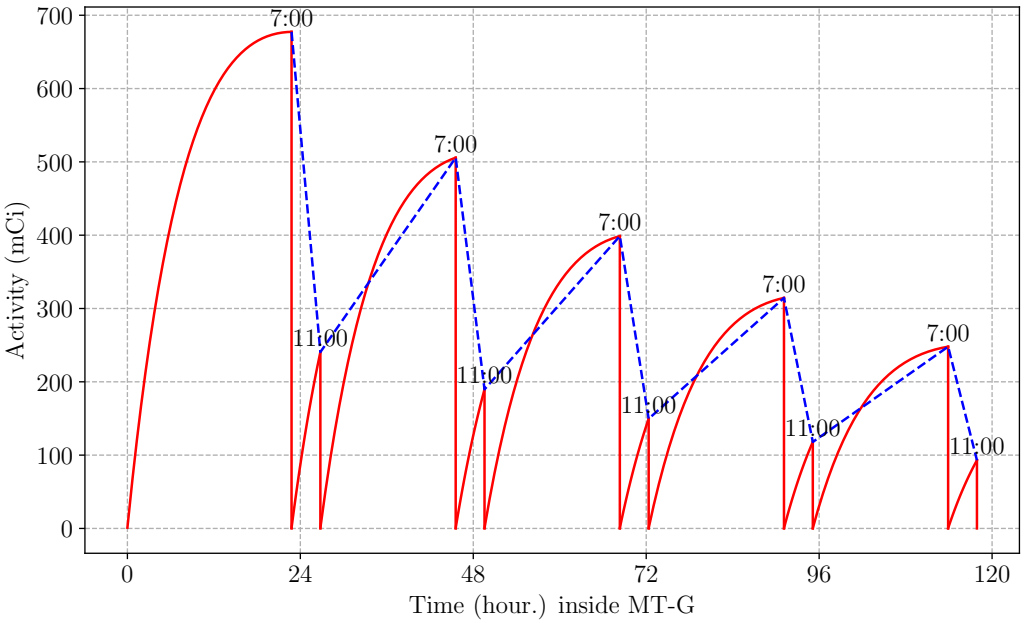

Figure 3: Optimal elution times by solving problem 7 ($q = 10$, $a_{M_0} = 1000$, and $h = 2$)

Constraint set 10 ensures that all patients are injected within their assigned eluted period. The technician is required to inject the radiopharmaceutical within time window $[t_k, t_k + l_k]$, $\forall k \in Q$, after which the radiopharmaceutical will not be effective due to the decay.

$$\begin{aligned} s_j^{(1)} &\geq \sum_{k \in Q} t_k x_{jk}, \quad \forall j \in J, \\ s_j^{(1)} &\leq \sum_{k \in Q} (t_k + l_k) x_{jk}, \quad \forall j \in J. \end{aligned} \tag{10}$$

Constraint set 11 ensures the precedence relations between any pair of patients in the injection stage,

$$\begin{aligned} &s_{j'}^{(1)} + b \leq s_j^{(1)} + c(1 - y_{j'j}^{(1)}), \quad \forall j, j' \in J : j \neq j', \\ &y_{j'j}^{(1)} + y_{jj'}^{(1)} = 1, \quad \forall j, j' \in J : j \neq j'. \end{aligned} \tag{11}$$

Equation set 12 denotes that the imposed scan completion time of patient j equals the sum of the start time of injection, duration of preparing and injecting the patient, preferred waiting time in the waiting room, and the duration of the scan.

$$d_j = s_j^{(1)} + b + w_j + p_j, \quad \forall j \in J. \tag{12}$$

The following constraint set (13) considers the precedence relation between the injection time and the scanning time.

$$s_j^{(1)} + b + w_j \leq s_j^{(2)}, \quad \forall j \in J. \tag{13}$$

Constraint set 14 assigns each patient to only one scanner according to set B_i,

$$\sum_{i \in I, j \in B_i} z_{ij} = 1, \quad \forall j \in J. \tag{14}$$

We also define a dummy patient, indexed with zero, in decision variable $y_{ijj'}^{(2)}$ to address the setup times. Note that this virtual patient does not play a role in computing the final completion time. Constraint set 15 ensures that at most one patient is scheduled as the first patient on each scanner after the dummy patient,

$$\sum_{j \in B_i} y_{i0j}^{(2)} \leq 1, \quad \forall i \in I. \tag{15}$$

Constraint set 16 maps the values of z_{ij} onto $y_{ijj'}^{(2)}$, i.e., the assignments to the precedence on scanners. This constraint set guarantees that every patient has exactly one successor and both are assigned to the same scanner. In other words, it establishes that every patient has precisely one predecessor and both are assigned to the same scanner.

$$z_{ij} = \sum_{j' \in B_i \cup \{0\} : j \neq j'} y_{ij'j}^{(2)}, \quad \forall i \in I, \forall j \in B_i. \tag{16}$$

Constraint set 17 decides the start times of scans according to the precedence relations and setup times.

$$\begin{aligned} & s_j^{(2)} + p_j + r(1 - o_{jj'}) \leq s_{j'}^{(2)} + c(1 - y_{ijj'}^{(2)}), \quad \forall i \in I,\ \forall j, j' \in B_i : j \neq j', \\ & \sum_{i \in I} \left(y_{ijj'} + y_{ij'j} \right) = 1, \quad \forall j, j' \in B_i : j \neq j'. \end{aligned} \tag{17}$$

Constraint set 17 does not assume any setup for the first scheduled patient on any scanner. If the procedures' protocol overrides this assumption, the following constraint must be activated,

$$s_j^{(2)} + c(1 - y_{i0j}^{(2)}) \geq r, \quad \forall j \in B_i. \tag{18}$$

Constraint set 19 preserves the linear structure of the earliness and the tardiness for scanning patients.

$$\begin{aligned} & T_j \geq s_j^{(2)} + p_j - d_j \geq 0, \quad \forall j \in J, \\ & E_j \geq dj - (s_j^{(2)} + p_j) \geq 0, \quad \forall j \in J. \end{aligned} \tag{19}$$

The objective function is defined as follows,

$$\textbf{minimize} \sum_{j \in J} (E_j + T_j). \tag{20}$$

6. Handling Uncertainty

In practice, efficiency variations of $\pm 20\%$ can occur in successive elutions of the same generator [1]. We assume that the behavior of the generator is predictable over time, i.e., we are able to efficiently estimate the current activity obtained in elution k by knowing the activity obtained in period $1, \ldots, k-1$. We capture and manage this uncertainty by applying a novel dynamic robust optimization approach.

6.1. Theory of Robust Optimization

Robust optimization (RO) is a tractable approach suited for problems in which parameters are unknown and their respective distributions are uncertain. In most real applications, a precise stochastic definition of uncertain events may not be available. This approach allows the decision-maker to encompass all realizations within the bounds of an uncertain parameter into special sets called "uncertainty sets." The goal is to guarantee the feasibility of constraints for the determined degree of realizations w.r.t. the worst-case criteria while optimizing an objective.

The original form of robust optimization, introduced by Soyster [19] and Falk [20], was generally concerned with linear programming problems with inexact coefficients in constraints. Their proposed robust optimization was subjected to be too conservative and it was limited to the column-wise structure. Plenty of studies have significantly generalized and extended the earlier models to the other classes of convex optimization problems beyond linear programming, e.g. conic and semi-definite programming (for example, see Ben-Tal and Nemirovski [21] and El Ghaoui et al. [22]). The other researches paved the way for a more complex description of the uncertainty polytopes, e.g., intersections of ellipsoidal uncertainty sets, budgeted uncertainty sets, et cetera. (for example, see Ben-Tal and Nemirovski [21] and Bertsimas and Sim [23]). The classical robust optimization approaches have had limitations in reducing the conservatism and increasing the reliability of the solutions. On the other hand, the classical uncertainty sets cannot capture the dynamics of the problems. In many important applications, notoriously in multi-period (dynamic) decision problems, some of the variables, which are called "wait and see" variables, can be determined after the uncertain parameter values (or a part of it) have been revealed. In other words, a part of the decision is postponed until more or full information on uncertain parameters has been obtained. This dynamic concept was named Adjustable Robust Optimization (ARO) by Ben-Tal et al. [24] (for a comprehensive review of extensions to ARO refer to Yanıkoğlu et al. [25]).

6.2. A novel dynamic approach

The key components of an uncertainty set are: nominal values of uncertain parameters, perturbation values, and the realization mechanism. In this study, the realization mechanism is recursively defined through the past events; we call the uncertainty set having this property a *monotone* uncertainty set and therefore, this type of uncertainty

set has a diminishing property over time. In other words, the cardinality of the set is limited upon receiving a realized parameter over time. In this section, we override the notation introduced earlier in section 3. Consider the following stochastic model,

$$\begin{aligned} \max_{x} \quad & f(x) \\ \text{s.t.} \quad & \sum_{j=1}^{n} \tilde{a}_{ij} x_j \leq \tilde{b}_i, \quad \forall i = 1, \dots, m, \\ & x \in \mathbb{R}_+, \end{aligned} \tag{21}$$

where $f(x)$ is a concave function in x. Parameters $\tilde{a}_{ij}$ and $\tilde{b}_i$ are not deterministic and their respective stochastic states are oscillating within a priori threshold, i.e., *support*, with unknown probability functions. Assume that $\tilde{a}_{ij} : [a_{ij} - \hat{a}_{ij}, a_{ij} + \hat{a}_{ij}] \xmapsto{\textbf{p.m.}} \xi_{ij} : [-1, +1]$ where **p.m.** stands for *parametrized mapping*. We also assume that the discrete support of the stochastic parameter produces a closed, finite, and countable set; i.e., the uncertainty set is a σ-algebra of Borel sets of its support. The above definitions also apply to $\tilde{b}_i$.

In this study, we recursively restrict the stochastic variable of the realization i, ξ_i, to the convex monotone combination of past realizations, i.e., $1, \dots, i-1$. By definition, the monotone uncertainty set is defined as follows,

$$\mathcal{U}_i = \begin{cases} \tilde{a}_{ij} = a_{ij} + \hat{a}_{ij}\xi_{ij}, \quad \forall j = 1, \dots, n, \\ \tilde{b}_i = b_i + \hat{b}_i \xi_{i0}, \\ \xi_{ij} = \sum_{i'=1}^{i-1} \gamma_{ij'} \xi_{ij'} \ : \ i \neq 1, \quad \forall j = 1, \dots, n, \qquad , \forall i = 1, \dots, m. \\ \xi_{i+1,j} \leq \xi_{ij} \ : \ i \neq m, \quad \forall j = 1, \dots, n, \\ \xi \in [-1, 1], \end{cases} \tag{22}$$

We impose the convexity-preserving variable, $\gamma_{ij'}$, in form of $\sum_{i=1}^{m} \gamma_{ij} = 1$ to the original model outside of the inner-maximization problem. Now, we apply the risk-averse approach to the uncertain parameters,

$$\begin{aligned} \max_{x} \quad & f(x) \\ \text{s.t.} \quad & \sum_{j=1}^{n} a_{ij} x_j + \max_{\xi_{ij} \in \mathcal{U}_i} \left\{ \sum_{j=1}^{n} \hat{a}_{ij} \xi_{ij} x_j + \hat{b}_i \xi_{i0} \right\} \leq b_i, \quad \forall i = 1, \dots, m, && (23) \\ & \sum_{i=1}^{m} \gamma_{ij} = 1, \quad \forall j = 1, \dots, n, && (24) \\ & x \in \mathbb{R}_+, \ \gamma \in [0, 1]. && (25) \end{aligned}$$

Theorem 6.1. *The robust counterpart w.r.t. $\mathcal{U}_i$ is deduced as a convex Quadratic-*

Constrained Problem (QCP).

$$
\begin{aligned}
\max_{x} \quad & f(x) \\
s.t. \quad & \sum_j a_{1j}x_j + \sum_j \left(\mu_{1j} + \mu'_{1j}\right) \leq b_1, && (26)\\
& \sum_j a_{ij}x_j + \sum_{i'=1}^{i-1}\sum_j \left(\mu_{i'j} + \mu'_{i'j}\right) \leq b_i, \quad \forall i = 2,\dots,m, && (27)\\
& \gamma_{1j}\left(\hat{a}_{2j}x_j + \hat{b}_2\right) - \mu_{1j} + \mu'_{1j} \leq 0, \quad \forall j = 1,\dots,n, && (28)\\
& \gamma_{1j}\left(\hat{a}_{ij}x_j + \hat{b}_i\right) - \mu_{1j} + \mu'_{1j} + \nu_{1j} \leq 0, && (29)\\
& \qquad \forall i = 3,\dots,m,\ \forall j = 1,\dots,n, \\
& \gamma_{ij}\left(\hat{a}_{i+1,j}x_j + \hat{b}_{i+1}\right) - \mu_{ij} + \mu'_{ij} - \nu_{i-1,j} \leq 0, && (30)\\
& \qquad \forall i = 2,\dots,m-1,\ \forall j = 1,\dots,n, \\
& \gamma_{i'j}\left(\hat{a}_{ij}x_j + \hat{b}_i\right) - \mu_{i'j} + \mu'_{i'j} - \nu_{i'-1,j} + \nu_{i'j} \leq 0, && (31)\\
& \qquad \forall i = 4,\dots,m-1,\ \forall i' = 2,\dots,i-2,\ \forall j = 1,\dots,n, \\
& \sum_{i=1}^{m}\gamma_{ij} = 1, \quad \forall j = 1,\dots,n, && (32)\\
& x, \mu, \mu', \nu, \nu' \in \mathbb{R}_+,\ \gamma \in [0,1]. && (33)
\end{aligned}
$$

Proof. Appendix A. □

The proposed strategy differs from classical AROs in different ways. First, we apply the dynamic nature of realization directly to the stochastic variable and the uncertain parameter. Second, we do not need to categorize the original variables into wait and see variables. Therefore, the original structure of the model remains intact.

6.3. Resource-encompassing constraints

An independent parameter is subjected to the uncertainty, i.e., the eluted `99mTc` at period k, v_k. We apply uncertainty set $\mathcal{U}_m$ to the constraints encompassing and affecting this parameter, constraint 9, as follows. Again, we aim to recursively estimate the value

of v_k by realizing its past values.

$$
\begin{aligned}
&\sum_{j\in J} \upsilon_j x_{j1} + \sum_{j\in J} \left(\mu_{1j} + \mu'_{1j}\right) \leq v_1,\\
&\sum_{j\in J} \upsilon_j x_{j1} + \sum_{k'=1}^{k-1} \sum_{j\in J} \left(\mu_{k'j} + \mu'_{k'j}\right) \leq v_k, \quad \forall k \in Q \setminus \{1\},\\
&\gamma_{1j}\hat{v}_2 - \mu_{1j} + \mu'_{1j} \leq 0, \quad \forall j \in J,\\
&\gamma_{1j}\hat{v}_k - \mu_{1j} + \mu'_{1j} + \nu_{1j} \leq 0, \quad \forall k \in Q \setminus \{1,2\},\ \forall j \in J,\\
&\gamma_{kj}\hat{v}_{k+1} - \mu_{kj} + \mu'_{kj} - \nu_{k-1,j} \leq 0, \quad \forall k \in Q \setminus \{2,q\},\ \forall j \in J,\\
&\gamma_{k'j}\hat{v}_k - \mu_{k'j} + \mu'_{k'j} - \nu_{k'-1,j} + \nu_{k'j} \leq 0, \quad \forall k \in Q \setminus \{1,2,3,q\},\ \forall k' = 2,\ldots,k-2,\ \forall j \in J,\\
&\sum_{k\in Q} \gamma_{kj} = 1, \quad \forall j \in J.
\end{aligned}
\tag{34}
$$

The resulting model by including constraints set 34 is a mixed integer linear program. Note that the duration of effective dosage for period k, l_k, is a dependent uncertain parameter and computed by a mapping parameter, α, after the realization of v_k, i.e., $l_k = \alpha v_k$. We replace constraint 9 with constraints set 34 and abbreviate the resulting model in Section 5 as $P(\mathcal{U}_m)$. We repeat the same process for the interval uncertainty set, $\mathcal{U}_\infty = \left\{\xi \mid \|\xi\| \leq 1\right\}$, and abbreviate the resulting model as $P(\mathcal{U}_\infty)$.

6.4. A posteriori analysis

Next, we introduce an a posteriori analysis framework to measure at which price the robust model based on the proposed uncertainty set delivers the objective values. We introduce a measure as a tradeoff between the degree of constraint violation against the value of the objective function under uncertainty. Hence, this is needed to be controlled. One strategy is that once the solution of the robust models is available, we compute the probability of the constraint violation based on the robust solution x^*. We use a measure proposed in [26] to compute the probability of constraint violation,

$$
\Pr\left\{\sum_{j=1}^{n} a_{ij}x_j^* + \sum_{j=1}^{n} \hat{a}_{ij}\xi_{ij}x_j^* > b_i\right\} \leq \exp\left(-\frac{d_i(x_j^*)^2}{\sum_{j=1}^{n} \hat{a}_{ij}^2 x_j^{*2}}\right), \quad \forall i = 1,\ldots,m, \tag{35}
$$

where $d_i(x) = b_i - \sum_{j=1}^{n} a_{ij}x_j - E\left[\sum_{j=1}^{n} \xi_{ij}\hat{a}_{ij}x_j\right]$. Without loss of generality, we can assume that ξ is independent and subject to a bounded probability distribution with a support on $[-1,1]$. We denote $\Lambda(\mathcal{U})$ the right-hand side of inequality 35. The less $\Lambda(\mathcal{U})$ is achieved, the worse objective values for the robust models, say $P(\mathcal{U}_\infty)$ and $P(\mathcal{U}_m)$, result. On the other hand, an α-protected solution of a problem is defined as the solution with the probability of violation less or equal than $(1-\alpha)\%$. Therefore, if a solution is not α-protected, it does not validate the desired uncertainty set and should be rejected.

7. Numerical Study

We emphasize a special case of the proposed formulation that is relevant to many diagnostic or imaging centers. In this context, we study the case of a molecular imaging center in the Shariati hospital located in Tehran, Iran. We study five most frequent procedures including the myocardial heart profusion scan (MIBI-H)[3], the bone scan (MDP)[4], the renal morphology, structure and function scan (DMSA)[5], the brain perfusion scan (ECD)[6], and the thyroid scintigraphy scan (MIBI-T)[7]. Six SPECT/CT (SC) scanners, SC-1 to SC-6, are distinguished in Table 2.

Table 2: Procedure/Scanner pair matrix

	SC-1	SC-2	SC-3	SC-4	SC-5	SC-6
MIBI-H				✓	✓	✓
MDP		✓	✓		✓	
DMSA		✓	✓			✓
ECD		✓			✓	
MIBI-T	✓	✓		✓	✓	

The scanning times per procedure are also different. Recall that the appointments are scheduled for one week ahead and approximately 30 patients are scanned in the center during a week. The generator is delivered on Saturday morning and they are expected to produce reasonable activity until Wednesday. The general constant parameters such as the injection time and the setup time, including the software configuration and changing the collimator, are considered 5 and 15 minutes, respectively. The other parameters are listed in Table 3.

Table 3: Procedures specifications

	MIBI-H	MDP	DMSA	ECD	MIBI-T
Frequency	51%	26%	7%	3%	13%
Scan duration (min.)	25	45	30	20	10
Waiting time (min.)	45	210	150	25	10
Activity required (mCi)	25	55	20	25	10

Example 2. Suppose that 30 patients are scheduled to receive the imaging services in a week. We assume that two elutions are allowed per day. Table 5 shows the type of

[3]A Myocardial Perfusion Imaging test shows how well blood flows through or perfuses the heart. It can show both the areas of the heart muscle that are not getting enough blood flow and how well the heart is pumping. This test is also known as a nuclear stress test.

[4]A common reason to obtain a bone scan (MDP) is in the evaluation of pain, in which a bone scan can help determine whether the source of the pain is from bone pathology or from the soft tissues.

[5]DMSA enters the kidneys and is concentrated in functioning/normal kidney tissue, giving an indication as to how the kidneys are working. It does not provide information as to the internal structure of the kidneys. In adults, reasons for having the test include looking for scars; estimating the function of both kidneys, particularly when planning kidney surgery; or for targeted treatment, such as radiotherapy.

[6]ECD SPECT scans are used to study the kinetics of the brain perfusion and other brain abnormalities.

[7]MIBI thyroid scintigraphy is a useful tool in differentiating malignant from benign thyroid nodules.

procedure of each patient. We compute parameters w_j and p_j for each $j \in J$ based on the procedures' parameters in Table 3. Table 4 reports the optimal elusion scenario for $a_{M_0} = 1000$, $q = 10$, and $h = 2$ according to the clinical aspects introduced in Section 4. Tables 6 and 7 report the allocation of patients to the alluted periods, x_{jk}, the scan starts, $s_j^{(2)}$, and imposed completion times, d_j, for models $P(\mathcal{U}_\infty)$ and $P(\mathcal{U}_m)$, respectively. According to Tables 6 and 7, we calculate the objective for $P(\mathcal{U}_\infty)$ as 275 minutes with $\Lambda(\mathcal{U}_\infty) = 2.71\%$, and the objective for $P(\mathcal{U}_m)$ as 211 minutes with $\Lambda(\mathcal{U}_\infty) = 4.33\%$. In other words, model $P(\mathcal{U}_\infty)$ delivers a schedule with 275 minutes total deviation from the imposed completion times. Model $P(\mathcal{U}_m)$ delivers it with 211 minutes deviation.

Table 4: Optimal elusion scenario for $a_{M_0} = 1000$, $q = 10$, and $h = 2$

k	1	2	3	4	5	6	7	8	9	10
t_k (min.)	1440	1620	2880	3060	4320	4500	5760	5940	7200	7560
v_k (mCi)	676.96	192.34	509.88	149.74	396.97	116.58	309.06	90.77	240.62	118.55

Table 5: Type of procedure per patient

Type of procedure	Index of patient (j)																											
	1	2	3	4	5	6	7	8	9	10	11	12	13	14	15	16	17	18	19	20	21	22	23	24	25	26	27	28	29	30
MIBI-H					✓	✓	✓								✓							✓				✓		✓		✓
MDP		✓						✓	✓	✓		✓		✓					✓					✓	✓		✓		✓	
DMSA													✓			✓	✓	✓			✓									
ECD	✓			✓																			✓							
MIBI-T			✓								✓									✓										

Table 6: Detailed output of $P(\mathcal{U}_\infty)$

j	l_k w.r.t. k										w_j	$s_j^{(2)}$ w.r.t. i						p_j	d_j
	1	2	3	4	5	6	7	8	9	10		1	2	3	4	5	6		
1	0	0	0	0	0	0	0	0	0	7560	50	0	7590	0	0	0	0	25	7610
2	0	0	0	0	0	0	0	0	7218	0	45	0	0	7433	0	0	0	35	7478
3	0	0	0	0	0	0	0	0	7228	0	30	7320	0	0	0	0	0	40	7253
4	0	0	0	0	0	0	0	0	7200	0	50	0	7230	0	0	0	0	25	7250
5	0	0	0	0	0	0	0	0	7223	0	60	0	0	0	0	7285	0	20	7298
6	0	0	0	0	0	0	0	0	7210	0	60	0	0	0	0	7260	0	20	7285
7	0	0	0	0	0	0	5770	0	0	0	60	0	0	0	5820	0	0	20	5845
8	0	0	0	0	0	0	0	5940	0	0	45	0	0	0	0	6155	0	35	6200
9	0	0	0	0	0	0	5788	0	0	0	45	0	0	0	0	6020	0	35	6048
10	0	0	0	0	0	0	5760	0	0	0	45	0	0	0	0	5975	0	35	6020
11	0	0	0	0	0	0	5765	0	0	0	30	5780	0	0	0	0	0	40	5790
12	0	0	0	0	0	4505	0	0	0	0	45	0	0	4720	0	0	0	35	4765
13	0	0	0	0	0	4500	0	0	0	0	50	0	0	0	0	0	4655	30	4685
14	0	0	0	0	4325	0	0	0	0	0	45	0	0	0	0	4540	0	35	4585
15	0	0	0	0	4320	0	0	0	0	0	60	0	0	0	4370	0	0	20	4395
16	0	0	0	0	4345	0	0	0	0	0	50	0	0	0	0	0	4500	30	4530
17	0	0	0	3088	0	0	0	0	0	0	50	0	0	0	0	0	3245	30	3273
18	0	0	0	3060	0	0	0	0	0	0	50	0	0	0	0	0	3215	30	3245
19	0	0	2890	0	0	0	0	0	0	0	45	0	0	0	0	3105	0	35	3150
20	0	0	0	3065	0	0	0	0	0	0	30	0	0	0	3080	0	0	40	3090
21	0	0	2880	0	0	0	0	0	0	0	50	0	0	0	0	0	3035	30	3065
22	0	0	2895	0	0	0	0	0	0	0	60	0	0	0	2945	0	0	20	2970
23	0	0	2885	0	0	0	0	0	0	0	50	0	0	0	0	2915	0	25	2935
24	0	1648	0	0	0	0	0	0	0	0	45	0	1880	0	0	0	0	35	1908
25	0	1620	0	0	0	0	0	0	0	0	45	0	1835	0	0	0	0	35	1880
26	0	1643	0	0	0	0	0	0	0	0	60	0	0	0	1755	0	0	20	1718
27	1468	0	0	0	0	0	0	0	0	0	45	0	0	0	0	1700	0	35	1728
28	1463	0	0	0	0	0	0	0	0	0	60	0	0	0	1520	0	0	20	1538
29	1440	0	0	0	0	0	0	0	0	0	45	0	0	0	0	1655	0	35	1700
30	1445	0	0	0	0	0	0	0	0	0	60	0	0	0	1495	0	0	20	1520

In the next comprehensive experiment, we design several test problems to measure the fluctuations in the objective values and degree of constraint violation by increasing in the

Table 7: Detailed output of $P(\mathcal{U}_m)$

j	l_k w.r.t. k										w_j	$s_j^{(2)}$ w.r.t. i						p_j	d_j
	1	2	3	4	5	6	7	8	9	10		1	2	3	4	5	6		
1	0	0	0	0	0	0	0	0	0	7560	50	0	7590	0	0	0	0	25	7610
2	0	0	0	0	0	0	0	0	7205	0	45	0	0	7420	0	0	0	35	7465
3	0	0	0	0	0	0	0	0	7220	0	30	7320	0	0	0	0	0	40	7245
4	0	0	0	0	0	0	0	0	7200	0	50	0	7230	0	0	0	0	25	7250
5	0	0	0	0	0	0	0	0	7215	0	60	0	0	0	0	7285	0	20	7290
6	0	0	0	0	0	0	0	0	7210	0	60	0	0	0	0	7260	0	20	7285
7	0	0	0	0	0	0	5770	0	0	0	60	0	0	0	0	5820	0	20	5845
8	0	0	0	0	0	0	0	5940	0	0	45	0	0	0	0	6155	0	35	6200
9	0	0	0	0	0	0	5780	0	0	0	45	0	0	0	0	6020	0	35	6040
10	0	0	0	0	0	0	5760	0	0	0	45	0	0	0	0	5975	0	35	6020
11	0	0	0	0	0	0	5765	0	0	0	30	5780	0	0	0	0	0	40	5790
12	0	0	0	0	0	4505	0	0	0	0	45	0	0	4720	0	0	0	35	4765
13	0	0	0	0	0	4500	0	0	0	0	50	0	4655	0	0	0	0	30	4685
14	0	0	0	0	4330	0	0	0	0	0	45	0	4545	0	0	0	0	35	4590
15	0	0	0	0	4325	0	0	0	0	0	60	0	0	0	0	4375	0	20	4400
16	0	0	0	0	4340	0	0	0	0	0	50	0	0	0	0	0	4505	30	4525
17	0	0	0	0	4320	0	0	0	0	0	50	0	0	0	0	0	4475	30	4505
18	0	0	0	3080	0	0	0	0	0	0	50	0	0	0	0	0	3235	30	3265
19	0	0	2900	0	0	0	0	0	0	0	45	0	0	0	0	3115	0	35	3160
20	0	0	0	3075	0	0	0	0	0	0	30	0	0	0	3090	0	0	40	3100
21	0	0	2880	0	0	0	0	0	0	0	50	0	0	0	0	0	3035	30	3065
22	0	0	2895	0	0	0	0	0	0	0	60	0	0	0	2945	0	0	20	2970
23	0	0	2885	0	0	0	0	0	0	0	50	0	2915	0	0	0	0	25	2935
24	0	1640	0	0	0	0	0	0	0	0	45	0	0	0	0	1880	0	35	1900
25	0	1620	0	0	0	0	0	0	0	0	45	0	0	0	0	1835	0	35	1880
26	0	1635	0	0	0	0	0	0	0	0	60	0	0	0	0	1755	0	20	1710
27	1455	0	0	0	0	0	0	0	0	0	45	0	0	0	0	1700	0	35	1715
28	1460	0	0	0	0	0	0	0	0	0	60	0	0	0	0	1520	0	20	1535
29	1440	0	0	0	0	0	0	0	0	0	45	0	0	0	0	1655	0	35	1700
30	1445	0	0	0	0	0	0	0	0	0	60	0	0	0	1495	0	0	20	1520

number of patients. We conduct this experiment on a Windows 10 64-bit machine with a core i7 2.66 GHz CPU and 12 GB memory. All mathematical models are coded and run on the Python 3.7 platform, including Gurobi 9 64-bit as the optimization engine. Table 8 reports the detailed configurations for the Gurobi engine. We follow the same process of Example 2 to generate a test problem.

Table 8: Gurobi parameters

`TimeLimit`	`3600 sec`
`MIPGapAbs`	`0.01`
`MIPFocus`	`2`
`Heuristics`	`0.2`
`PreCrush`	`1`
`Cuts`	`3`

Each experiment is based upon the number of patients and contains 20 test problems. Figure 4 illustrates the descriptive statistics of the objective value including the mean and the maximum of test problems. It is clear that the mean and max objective values of $P(\mathcal{U}_m)$ outperform those of $P(\mathcal{U}_\infty)$. One practical question is that at most how many patients can be scanned in the real situation. The current total deviation from the imposed scan completion times is about $30 \times 25 = 750$ minutes for 30 patients. The mean deviations for $P(\mathcal{U}_m)$ and $P(\mathcal{U}_\infty)$ are 156 and 335 minutes for this number of patients. The overall objective value for $P(\mathcal{U}_m)$ is approximately 42% better than that of $P(\mathcal{U}_\infty)$. However, the mean deviations for $P(\mathcal{U}_m)$ and $P(\mathcal{U}_\infty)$ are 3484 and 5237 minutes for 55 patients. Considering $P(\mathcal{U}_m)$, each patient should incur approximately 63 minutes

deviation from its dedicated imposed scan completion time. Hence, according to $P(\mathcal{U}_m)$ and $P(\mathcal{U}_\infty)$, it is not plausible to schedule 55 number of patients within a week. This range of deviation dramatically increases the waiting times and decreases the customer satisfaction.

On the other hand, there exists a theoretical reason not to schedule patients up to a specific threshold. Figure 5 shows that under 0.95-protected solution, $\alpha = 0.05$, it is acceptable to scan at most 40 patients since the degree of constraint violation drastically increases after this threshold. It is natural that the degree of violation of $P(\mathcal{U}_\infty)$ is less than that of $P(\mathcal{U}_m)$ since $P(\mathcal{U}_\infty)$ is a risk-averse approach. On the other hand, Figure 5 validates the realistic concept of the monotone uncertainty set since it controls the constraint violation up to a specific threshold under 0.95-protected and 0.9-protected solutions.

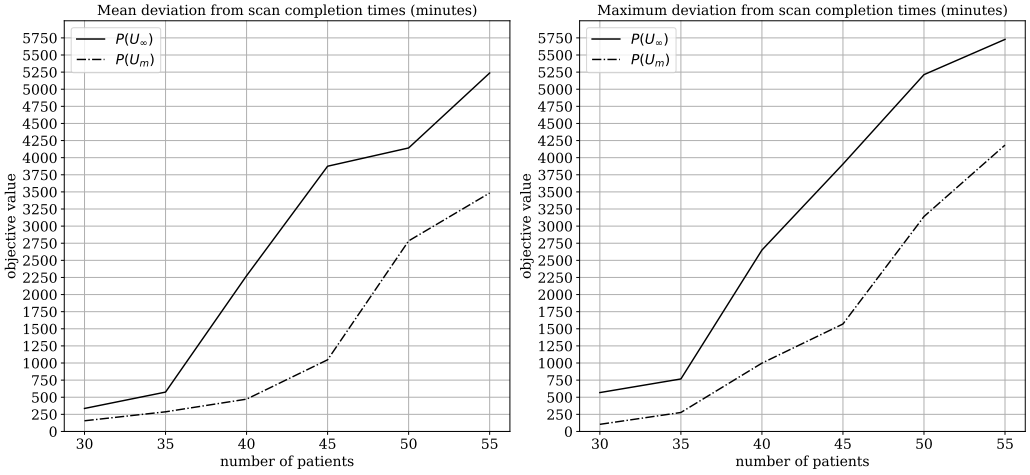

Figure 4: Comparison of objective values of robust models

Figure 6 reports the percentage of patients scanned exactly at their imposed scan completion times, percentage of deviation, and percentage of patients scanned with 10 minutes tolerance from their imposed scan completion times. The second figure is practically a clinical opportunity and often creates more flexibility in the final schedules. For example, considering 30 patients, the percentage of deviations are about 10 and 2 percent without and with 10 minutes tolerance, respectively. This figure also validates our prior conclusion that the acceptable range for scanning patients is about 30 to 40 during a week.

8. Conclusion

Administrating resources in a medical imaging center and coordinating them with the scheduling of outpatients may be difficult to quantify since it depends on the types of resources and the protocols for the procedures. On the other hand, the tactical and operational scheduling decisions for a medical imaging center may not be suitable

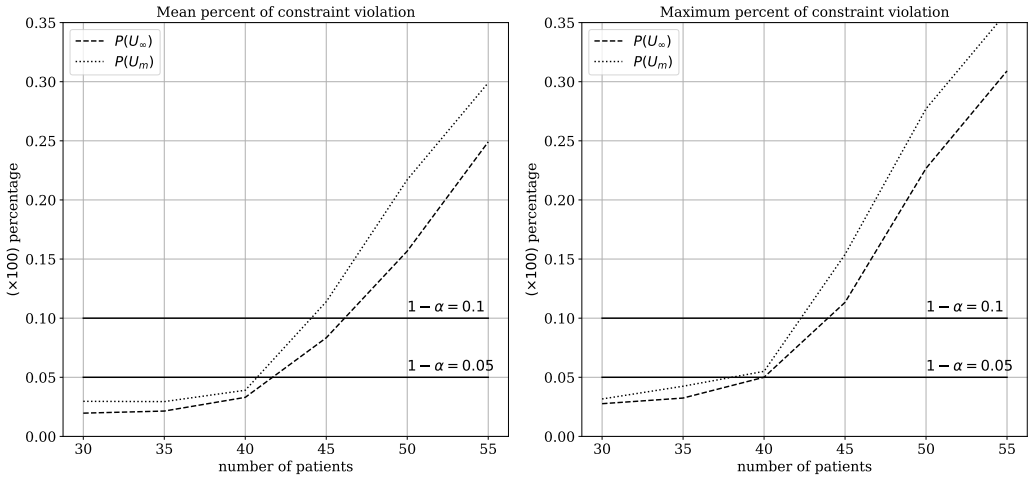

Figure 5: Comparison of degree of constraint violations of robust models

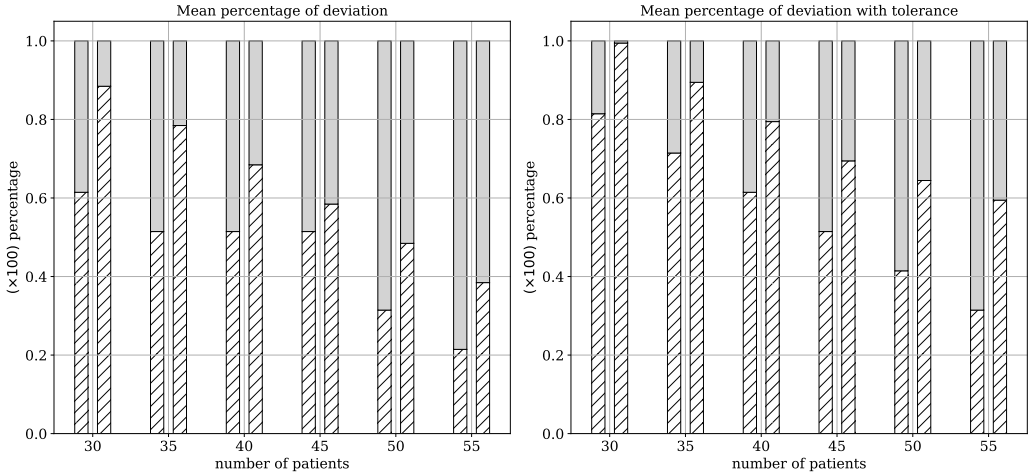

Figure 6: Percentage of violation from scheduled scan times (left bar: $P(U_\infty)$, right bar: $P(U_m)$), grey colour: not on time, patched lines: on time

for another. In this study, we attempt to generalize several clinical concepts for both pharmaceutical assignment and scheduling appointments and build a general mathematical framework to cope with the primary requirements of a medical imaging center.

We studied the case of a molecular imaging center in the Shariati hospital located in Tehran, Iran. We studied five essential and most frequent procedures processed on six different scanners. In our case study, the appointments were scheduled for one week ahead and we concluded that about 30 to 40 patients can be scanned in the center with the percentage of violation from scanned time 2 to 10 percents during a week. To achieve

these figures, we proposed a dynamic and realistic robust optimization framework by overriding the worst-case criterion and decreasing the support of the uncertainty set by realizing the previous states of available resources.

We conclude this section with three future research directions. First, emergency outpatients often disturb the predefined appointments both through the injection and preparation stage and the scanning stage. This disturbance decreases the quality of schedules. Second, batching outpatients based on the type of the procedures can be an efficient approach to reduce the setup times. Third, the connection of the scheduling decision module with the artificial intelligence-directed quality assurance module of scanned images is another option to certify obtaining better interpretable images.

Appendix A.

Proof. (Theorem 6.1)

Proof by induction. We construct the dual of the inner maximization expression in constraint 23, the primal problem, in form $D(i)$, $\forall i \in \{1, \ldots, m\}$. Note that dual variables μ_{ij} are defined on the primal constraints including only one variable and dual variables ν_{ij} are defined on the primal constraints including two variables. Since the primal problem is non-empty and bounded, the dual problem should have a bounded optimum according to the strong dual theorem.

$$\begin{aligned} \mathrm{D}(i=1): \min_{\mu,\nu} \quad & \left\{ \sum_j \left(\mu_{1j} + \mu'_{1j} \right) \right\} \\ \text{subject to} \quad & \mu_{1j} - \mu'_{1j} \geq \hat{a}_{1j} x_j, \quad \forall j. \end{aligned}$$

$$\begin{aligned} \mathrm{D}(i=2): \min_{\mu,\nu} \quad & \left\{ \sum_j \left(\mu_{1j} + \mu'_{1j} \right) \right\} \\ \text{subject to} \quad & \mu_{1j} - \mu'_{1j} \geq \gamma_{1j} \hat{a}_{2j} x_j, \quad \forall j. \end{aligned}$$

$$\begin{aligned} \mathrm{D}(i=3): \min_{\mu,\nu} \quad & \left\{ \sum_j \left(\mu_{1j} + \mu'_{1j} + \mu_{2j} + \mu'_{2j} \right) \right\} \\ \text{subject to} \quad & \mu_{1j} - \mu'_{1j} - \nu_{1j} \geq \gamma_{1j} \hat{a}_{3j} x_j, \quad \forall j, \\ & \mu_{2j} - \mu'_{2j} + \nu_{1j} \geq \gamma_{2j} \hat{a}_{3j} x_j, \quad \forall j. \end{aligned}$$

$$
\begin{aligned}
\mathrm{D}(i=4): \min_{\mu,\nu} \quad & \left\{ \sum_j \left(\mu_{1j} + \mu'_{1j} + \mu_{2j} + \mu'_{2j} + \mu_{3j} + \mu'_{3j} \right) \right\} \\
\text{subject to} \quad & \mu_{1j} - \mu'_{1j} - \nu_{1j} \geq \gamma_{1j} \hat{a}_{4j} x_j, \quad \forall j, \\
& \mu_{2j} - \mu'_{2j} + \nu_{1j} - \nu_{2j} \geq \gamma_{2j} \hat{a}_{4j} x_j, \quad \forall j, \\
& \mu_{3j} - \mu'_{3j} + \nu_{2j} \geq \gamma_{3j} \hat{a}_{4j} x_j, \quad \forall j.
\end{aligned}
$$

$$
\begin{aligned}
\mathrm{D}(i=m): \min_{\mu,\nu} \quad & \left\{ \sum_{i'=1}^{i-1} \sum_j \left(\mu_{i'j} + \mu'_{i'j} \right) \right\}, \quad \forall i = 1, \ldots, m, \\
\text{subject to} \quad & \gamma_{1j} \left(\hat{a}_{2j} x_j + \hat{b}_2 \right) - \mu_{1j} + \mu'_{1j} \leq 0, \quad \forall j = 1, \ldots, n, \\
& \gamma_{1j} \left(\hat{a}_{ij} x_j + \hat{b}_i \right) - \mu_{1j} + \mu'_{1j} + \nu_{1j} \leq 0, \\
& \qquad \forall i = 3, \ldots, m, \ \forall j = 1, \ldots, n, \\
& \gamma_{ij} \left(\hat{a}_{i+1,j} x_j + \hat{b}_{i+1} \right) - \mu_{ij} + \mu'_{ij} - \nu_{i-1,j} \leq 0, \\
& \qquad \forall i = 2, \ldots, m-1, \ \forall j = 1, \ldots, n, \\
& \gamma_{i'j} \left(\hat{a}_{ij} x_j + \hat{b}_i \right) - \mu_{i'j} + \mu'_{i'j} - \nu_{i'-1,j} + \nu_{i'j} \leq 0, \\
& \qquad \forall i = 4, \ldots, m-1, \ \forall i' = 2, \ldots, i-2, \ \forall j = 1, \ldots, n.
\end{aligned}
$$

□

References

[1] A. C. Perkins, G. Vivian, Molybdenum supplies and nuclear medicine services, 2009.

[2] A. Nagurney, L. S. Nagurney, Medical nuclear supply chain design: A tractable network model and computational approach, International Journal of Production Economics 140 (2012) 865–874.

[3] A. J. Einstein, Breaking america's dependence on imported molybdenum, JACC: Cardiovascular Imaging 2 (2009) 369–371.

[4] S. Suthummanon, V. K. Omachonu, M. Akcin, Applying activity-based costing to the nuclear medicine unit, Health services management research 18 (2005) 141–150.

[5] M. Andersson, S. Mattsson, Dose management in conventional nuclear medicine imaging and pet, Clinical and Translational Imaging 4 (2016) 21–30.

[6] A. Nagurney, L. S. Nagurney, Medical nuclear supply chain design: A tractable network model and computational approach, International Journal of Production Economics 140 (2012) 865–874.

[7] A. Nagurney, L. S. Nagurney, D. Li, Securing the sustainability of global medical nuclear supply chains through economic cost recovery, risk management, and optimization, International Journal of Sustainable Transportation 9 (2015) 405–418.

[8] E. Pérez, L. Ntaimo, C. O. Malavé, C. Bailey, P. McCormack, Stochastic online appointment scheduling of multi-step sequential procedures in nuclear medicine, Health care management science 16 (2013) 281–299.

[9] E. Pérez, L. Ntaimo, W. E. Wilhelm, C. Bailey, P. McCormack, Patient and resource scheduling of multi-step medical procedures in nuclear medicine, IIE Transactions on Healthcare Systems Engineering 1 (2011) 168–184.

[10] E. Pérez, L. Ntaimo, C. Bailey, P. McCormack, Modeling and simulation of nuclear medicine patient service management in devs, Simulation 86 (2010) 481–501.

[11] E. P. Roman, Simulation and optimization models for scheduling multi-step sequential procedures in nuclear medicine, Texas A&M University, 2010.
[12] F. Akhavizadegan, J. Ansarifar, F. Jolai, A novel approach to determine a tactical and operational decision for dynamic appointment scheduling at nuclear medical center, Computers & Operations Research 78 (2017) 267–277.
[13] J. Patrick, M. L. Puterman, Improving resource utilization for diagnostic services through flexible inpatient scheduling: A method for improving resource utilization, Journal of the Operational Research Society 58 (2007) 235–245.
[14] J. Patrick, M. L. Puterman, M. Queyranne, Dynamic multipriority patient scheduling for a diagnostic resource, Operations research 56 (2008) 1507–1525.
[15] L. V. Green, S. Savin, B. Wang, Managing patient service in a diagnostic medical facility, Operations Research 54 (2006) 11–25.
[16] B. P. Berg, B. T. Denton, Fast approximation methods for online scheduling of outpatient procedure centers, INFORMS Journal on Computing 29 (2017) 631–644.
[17] V. P. Chechev, M.-M. Bé, Radioactive equilibrium: 99mo/99mtc decay characteristics, Applied Radiation and Isotopes 87 (2014) 132–136.
[18] H. D. Sherali, C. Shetty, M. Bazaraa, Nonlinear programming: Theory and algorithms, Wiley-Interscience, 2006.
[19] A. L. Soyster, Convex programming with set-inclusive constraints and applications to inexact linear programming, Operations research 21 (1973) 1154–1157.
[20] J. E. Falk, Exact solutions of inexact linear programs, Operations Research 24 (1976) 783–787.
[21] A. Ben-Tal, A. Nemirovski, Robust convex optimization, Mathematics of operations research 23 (1998) 769–805.
[22] L. El Ghaoui, F. Oustry, H. Lebret, Robust solutions to uncertain semidefinite programs, SIAM Journal on Optimization 9 (1998) 33–52.
[23] D. Bertsimas, M. Sim, The price of robustness, Operations research 52 (2004) 35–53.
[24] A. Ben-Tal, A. Goryashko, E. Guslitzer, A. Nemirovski, Adjustable robust solutions of uncertain linear programs, Mathematical programming 99 (2004) 351–376.
[25] İ. Yanıkoğlu, B. L. Gorissen, D. den Hertog, A survey of adjustable robust optimization, European Journal of Operational Research 277 (2019) 799–813.
[26] Z. Li, Q. Tang, C. A. Floudas, A comparative theoretical and computational study on robust counterpart optimization: Ii. probabilistic guarantees on constraint satisfaction, Industrial & engineering chemistry research 51 (2012) 6769–6788.